

Drying dissipative structures of the thermosensitive gels of poly(*N*-isopropyl acrylamide) on a cover glass

Tsuneo Okubo · Emi Itoh · Akira Tsuchida ·
Etsuo Kokufuta

Received: 15 July 2006 / Accepted: 19 August 2006 / Published online: 19 October 2006
© Springer-Verlag 2006

Abstract Drying dissipative structural patterns of the thermosensitive gels of poly(*N*-isopropyl acrylamide) were studied on a cover glass. As the temperature of suspension and room rose from 25 to 50 °C, the small size of drying pattern area extended to the beautiful flickering spoke-like ones transitionally at the critical temperature ca. 35 °C. The principal patterns at 25 °C were the single or multiple broad rings of the hill accumulated with the gels. At 50 °C, on the other hand, the flickering spoke-like patterns were observed at the inner area of the broad ring especially at the gel concentrations higher than 1×10^{-3} g/ml. These observations support that the extended gels at low temperatures apt to associate weakly to each other, whereas the gels at high temperatures shrink and move rather freely with the convective flow of water, though the very weak intergel attractions still remain. In the presence of sodium chloride at high temperatures, the cooperative patterns formed between the gel spheres and the salt. The gravitational and Marangoni convective flow of the gels and the very

weak interactions between the gels and substrate (cover glass) are important for the flickering spoke-like pattern formation.

Keywords Drying dissipative pattern · Convection · Thermosensitive gel · Poly(*N*-isopropyl acrylamide) · Flickering spoke-like pattern

Introduction

Generally speaking, most structural patterns in nature form via self-organization accompanied with the dissipation of free energy and in the nonequilibrium state. Among several factors in the free energy dissipation, evaporation at the liquid surface and gravitational and Marangoni convections are very important. To understand the mechanism of the dissipative self-organization of the simple model systems instead of the much complex nature itself, the authors started to study the *convective*, *sedimentation*, and *drying* dissipative patterns of colloidal suspensions as systematically as possible.

In previous papers from our laboratory [1, 2], *drying* dissipative patterns on a cover glass have been studied for colloidal crystal suspensions of silica and polystyrene spheres. Quite similar macroscopic and microscopic structural patterns formed between the two kinds of spheres. The broad ring patterns of the hill accumulated with spheres in the outside edges and the spoke-like and ring-like cracks formed in the macroscopic scale. The existence of the small circle-like convection cells proposed by Terada et al. [3–6] was supported. Furthermore, influence of colloidal size ranging on the drying patterns of colloidal crystal has been clarified [7]. Structural patterns were observed in the course of drying Chinese black ink on a cover glass and in a dish

T. Okubo
Institute for Colloidal Organization,
Hatoyama 3-1-112, Uji,
Kyoto 611-0012, Japan

T. Okubo (✉)
Cooperative Research Center, Yamagata University,
Johnan 4-3-16,
Yonezawa 992-8510, Japan
e-mail: okubotsu@ybb.ne.jp

E. Itoh · A. Tsuchida
Department of Applied Chemistry, Gifu University,
Gifu 501-1193, Japan

E. Kokufuta
Institute of Applied Biochemistry, University of Tsukuba,
Tsukuba 305-8572, Japan

[8]. The clear broad ring and spoke-like patterns of the rims formed in the outside edges and in the central region of the film, respectively. It is interesting to note that the primitive vague patterns of valleys were formed already in the concentrated suspensions before dryness and they grew toward fine cracks in the course of solidification. Branch-like fractal patterns of the sphere association were observed in the microscopic scale. The macroscopic drying patterns of the fractionated and monodispersed bentonite particles (plate-like in their shape) coexisted with the broad ring and the round hill accumulated with the particles around the outside edges of the film and in the center area, respectively, in the macroscopic scale [9]. By the addition of NaCl, the pattern shifted from the broad ring to the round hill. The spoke-like cracks, which have been observed for the spheres so often hitherto, were not observed for the bentonite particles at all. Wrinkled, branch-like and/or star-like fractal patterns were observed in the microscopic scale.

The drying patterns have been studied further for the linear-type macrocations, i.e., poly(allylamine hydrochloride) [10]. Macroscopic broad ring patterns were formed. Furthermore, beautiful string-like fractal patterns were observed in the microscopic scale. Drying patterns of poly(ethylene glycol) having molecular weights ranging from 1,000 to 2×10^6 in aqueous solution have been also studied on a cover glass [11]. In addition of the macroscopic broad rings, the single round hills formed in the center, when the molecular weight was large. Cross-like fractal patterns appeared, especially for the diluted solutions in the microscopic scale. The drying experiments were made for cationic detergent of *n*-dodecyltrimethylammonium chloride [12]. Recently, a series of anionic detergent molecules, sodium *n*-alkyl sulfates (*n*-alkyl = *n*-hexyl, *n*-octyl, *n*-decyl, *n*-dodecyl, *n*-hexadecyl, and *n*-octadecyl) were used for study of the drying dissipative patterns [13]. Broad ring patterns formed in the macroscopic scale. Star-like, branch-like, arc-like, and small block-like microstructures were also observed. The convection of water and the detergent molecules at different rates under gravity and the translational and rotational Brownian movement of the latter were important for the macroscopic pattern formation. Microscopic patterns also formed by the translational Brownian diffusion of the detergent molecules and the electrostatic and the hydrophobic interactions between detergents and/or between the detergents and substrate in the course of the solidification. Recently, macroscopic and microscopic drying patterns of a series of aqueous solutions of polyoxyethylenealkyl ethers were studied [14]. The shift from the single round hill of accumulated surfactant molecules with rough surface to the broad ring patterns of the hill with the smooth surface occurred as the HLB (hydrophile-lyophile balance) of the surfactants increased.

From these studies on drying structures, very similar macroscopic broad ring patterns formed irrespective of kind of solutes and their concentrations. Microscopic drying patterns such as branch-like, string-like, arc-like, and small block-like ones were, however, reflected from the shape, size, and flexibility of the solute molecules.

Quite recently, the *sedimentation* dissipative patterns formed in the course of drying colloidal silica spheres and green tea (Ocha) have been studied in a glass dish and in a watch glass, for example [15–17]. The broad ring patterns were formed within several 10 min in suspension state by the *convectioal* flow of water and the colloidal particles. The sedimentary particles were suspended above the substrate and always moved by the external fields including convectioal flow. The convectioal dissipative structures were also studied for the 100% ethanol suspensions of colloidal silica spheres [18]. Vigorous cell convectioal flow was observed with the naked eyes, and the patterns changed dynamically with time. In this work, drying dissipative patterns of the thermosensitive gels, poly(*N*-isopropyl acrylamide) were studied. Unexpectedly, the authors observed the characteristic thermosensitive change in the drying patterns.

Experimental

Materials

Poly(*N*-isopropyl acrylamide) gel spheres (PNIPAAm) were prepared in the same manner as described in the previous papers [19, 20]. The gel concentrations ranged from 1×10^{-11} to 0.02 g/ml. The size of PNIPAAm gel spheres was evaluated from the DLS measurements between 15 and 55 °C [21]. The hydrodynamic diameter decreased from 72 nm at 20 °C to 28 nm at 50 °C, which corresponds to a volume change by a factor of 17. The diameter decreased transitionally at ca. 35 °C. The size changed reversibly when the temperature increased and then decreased [21]. The water used for the sample purification and preparation was purified by a Milli-Q reagent grade system (Milli-RO5 plus and Milli-Q plus, Millipore, Bedford, MA, USA).

Observation of the drying dissipative structures

Approximately 0.05 ml of the aqueous suspension of PNIPAAm gels was dropped carefully and gently on a micro cover glass (30×30 mm, thickness No. 1, 0.12 to 0.17 mm, Matsunami Glass, Kishiwada, Osaka, Japan) in a dish (60 mm in diameter, 15 mm in depth, Petri, Tokyo, Japan). The cover glass was used without further rinsing in this work. The extrapolated value of the contact angle for

pure water was $31 \pm 0.2^\circ$ from the drop profile of a small amount of water (0.2, 0.4, 0.6, and 0.8 μl) on the cover glass. A pipet (1 ml, disposable serological pipet, Corning Lab. Sci.) was used for the dropping. Observation of the macroscopic and microscopic drying patterns was made for the film formed after the suspension was dried up completely on a cover glass in a room air-conditioned at 25°C and 65% in humidity of the air. Macroscopic dissipative structures were observed with a digital HD microscope (type VH-7000, Keyence, Osaka Japan) and a Canon EOS 10 camera with macrolens (EF 50 mm, $f=2.5$) and a life-size converter EF. Microscopic structures and the thickness profiles of the dried film were observed with a laser 3D profile microscope (type VK-8500, Keyence), a digital microscope (type VHX-500, Keyence) and a metallurgical microscope (Axiovert 25CA, Carl-Zeiss, Jena GmbH).

Results and discussion

Influence of the gel concentration

Figure 1 show the typical patterns formed in the course of drying the suspensions of PNIPAAm gel spheres at 25°C and at the gel concentrations ranging from 1×10^{-11} to 0.02 g/ml. The small broad ring patterns were always observed in the central part of the initial suspension area irrespective of gel concentrations. Two causes are considered for the small film formation of gel spheres; one is the rather large contact angle between the gel suspension and the substrate at 25°C and the suspension area moved to the

central part of the initial suspension area when the suspension is concentrated by the evaporation of water molecules with time. The other, probably main cause will be due to the weak entanglement of the extended gels in the course of the concentration processes resulted in the accumulation of the gels in the central area only. A main cause for the broad ring formation in the small film is due to the convection flow of water and the gel spheres in the different rates, where the rate of the latter is much slower than that of the former under gravity. Especially, flow of the gels from the center area toward the outside edges in the lower layer of the liquid drop, which was observed on a digital HD microscope directly from the movement of the very rarely occurred aggregates of the particles, is important [8]. The convectational flow is enhanced by the evaporation of water at the air–liquid surface, resulting to the lowering of the temperature in the upper region of the suspension. When the gel spheres reach the edges of the drying frontier at the outside region of the liquid, a part of the gels will turn upward and go back to the center region. However, the movement of most gels may stop at the frontier region by the disappearance of water. This process must be followed by the broad ring accumulation of the gels near the round edges. It should be noted that the broad ring formation in the drying patterns has been observed for most of the suspensions and solutions examined by our group [1, 2, 7–14] and further by other researchers [22–24]. Recently, microgravity experiments were made for the observation of the drying dissipative patterns of deionized suspension of colloidal silica spheres (Tsuchida et al., publication in preparation). It is surprising to note that the broad ring patterns did not disappear even in microgravity. This

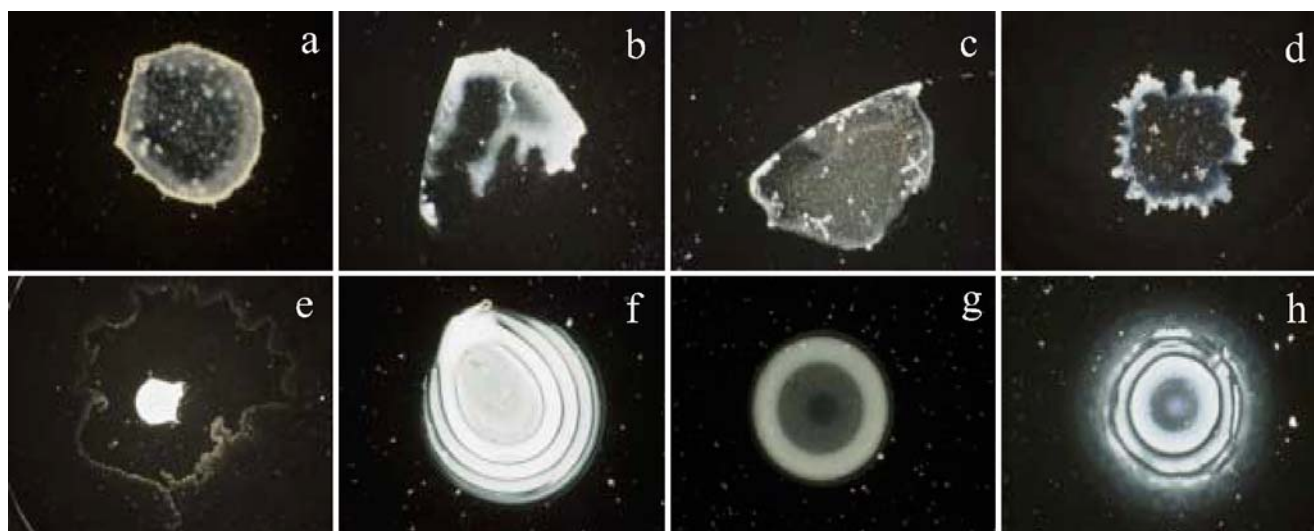


Fig. 1 Drying patterns of PNIPAAm at 25°C . In water, 0.05 ml, **a** $w=1.0 \times 10^{-11}$ g/ml, **b** 1.0×10^{-9} g/ml, **c** 1.0×10^{-7} g/ml, **d** 1.0×10^{-5} g/ml, **e** 1.0×10^{-3} g/ml, **f** 7.5×10^{-3} g/ml, **g** 0.01 g/ml, and **h** 0.02 g/ml; length of the bar is 0.5 mm

supports that both the gravitational and Marangoni convections contribute for the broad ring formation on earth but the latter is still important in microgravity. Quite recently, the authors observed that the broad rings were formed already in the sedimentation patterns in the liquid phase [15, 16]. The film surfaces were rough, as observed with the naked eyes in the low gel concentrations, whereas they came to be smooth and the single and multiple broad rings were formed especially above 7.5×10^{-3} g/ml (see Fig. 1).

Figure 2 shows the thickness of the dried film of PNIPAAm formed at 25 °C. Clearly, there appeared a round hill in the center region in addition of the broad ring in the outside edges. These hills in the central area have not been observed for the suspensions of any kind of spherical particles hitherto. The rotational movement must be highly restricted for the gel spheres because they are hairy, very soft, interactive with the substrate, and the restricted sliding movement will be major especially in the area close to the substrate plane. This restricted Brownian movement must be correlated deeply to the appearance of the hill in the center area. Similar hill formation has been observed for the anisotropic-shaped particles like plate-like fractionated bentonite particles [9].

Influence of temperature

Figure 3 shows the drying patterns at the lowest gel concentration of $w=1.0 \times 10^{-5}$ g/ml and at various temperatures ranging from 25 to 45 °C. It is surprising to note that the patterns changed drastically when the temperature rose above the transition temperature. Above the transition temperature, around 35 °C, patterns spread widely and multiple broad rings were observed as is shown in

subpanels b–d of Fig. 3. Measurements of the thickness of the film dried showed only the single broad ring in the outside area of the film, though the film formed from the suspension at $w=1 \times 10^{-5}$ g/ml was too thin, smaller than 1 μm , to estimate the thickness precisely. Extension of the drying patterns above the 35 °C supports the fact that the gel spheres at higher temperatures than 35 °C shrink and becomes rather hard compared with the extended and soft ones at 25 °C below the transition temperature. Thus, it is highly plausible that the spheres at high temperatures are now able to move much easily both transitionally and rotationally. However, the gel spheres at high temperatures still cannot move so freely compared with the typical solid spheres like colloidal silica and polystyrene spheres. Affinitive interactions inducing very slight entanglement between the neighbored gel spheres may still remain because the surfaces of the gels must be still covered with the soft and linear-type single chains of PNIPAAm.

Figure 4 shows the drying patterns as a function of the temperatures when the gel concentration increased at $w=1 \times 10^{-3}$ g/ml, 100-fold high compared with that of Fig. 3. Now, the pattern extension covering whole the initial suspension area is clear above the transition temperature. The broad rings, fine multiple rings, and spoke-like patterns are clearly observed at high temperatures (see subpanels c, g, d and h of Fig. 3). It should be mentioned in this study that these patterns were also observed clearly for Chinese ink [8], which is made from soot and glue and has been used for writing for a long time in China and Japan. These colloidal particles are called protective colloids and composed of the hydrophobic carbon spheres covered with hydrophilic glue. Thus, Chinese ink and PNIPAAm gels at high temperatures are similar to each other in the characters of affinitive interactions between the gels.

Fig. 2 Thickness of the dried film of PNIPAAm at 25 °C. In water, 0.05 ml, **a** $w=1.0 \times 10^{-5}$ g/ml, **b** 5.0×10^{-4} g/ml, **c** 1×10^{-3} g/ml, **d** 7.5×10^{-3} g/ml, **e** 0.01 g/ml, and **f** 0.02 g/ml

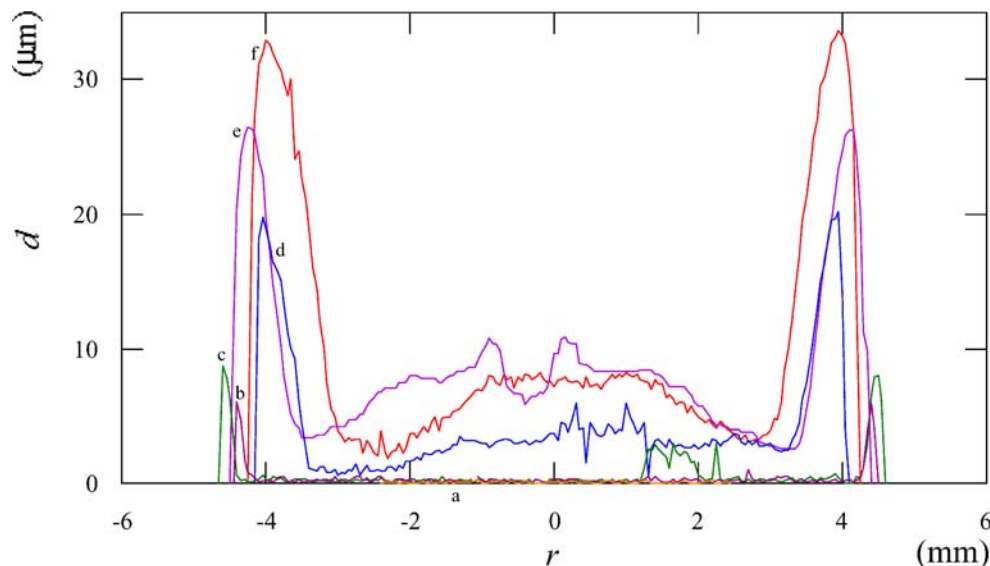


Fig. 3 Drying patterns of PNIPAAm at 25 °C. In water, 0.05 ml, $w=1.0 \times 10^{-5}$ g/ml, **a** and **e** 25 °C, **b** and **f** 35 °C, **c** and **g** 40 °C, **d** and **h** 45 °C; length of the bar is 2.0 mm for **a**, **b**, **c**, and **d** and 0.5 mm for **e**, **f**, **g**, and **h**

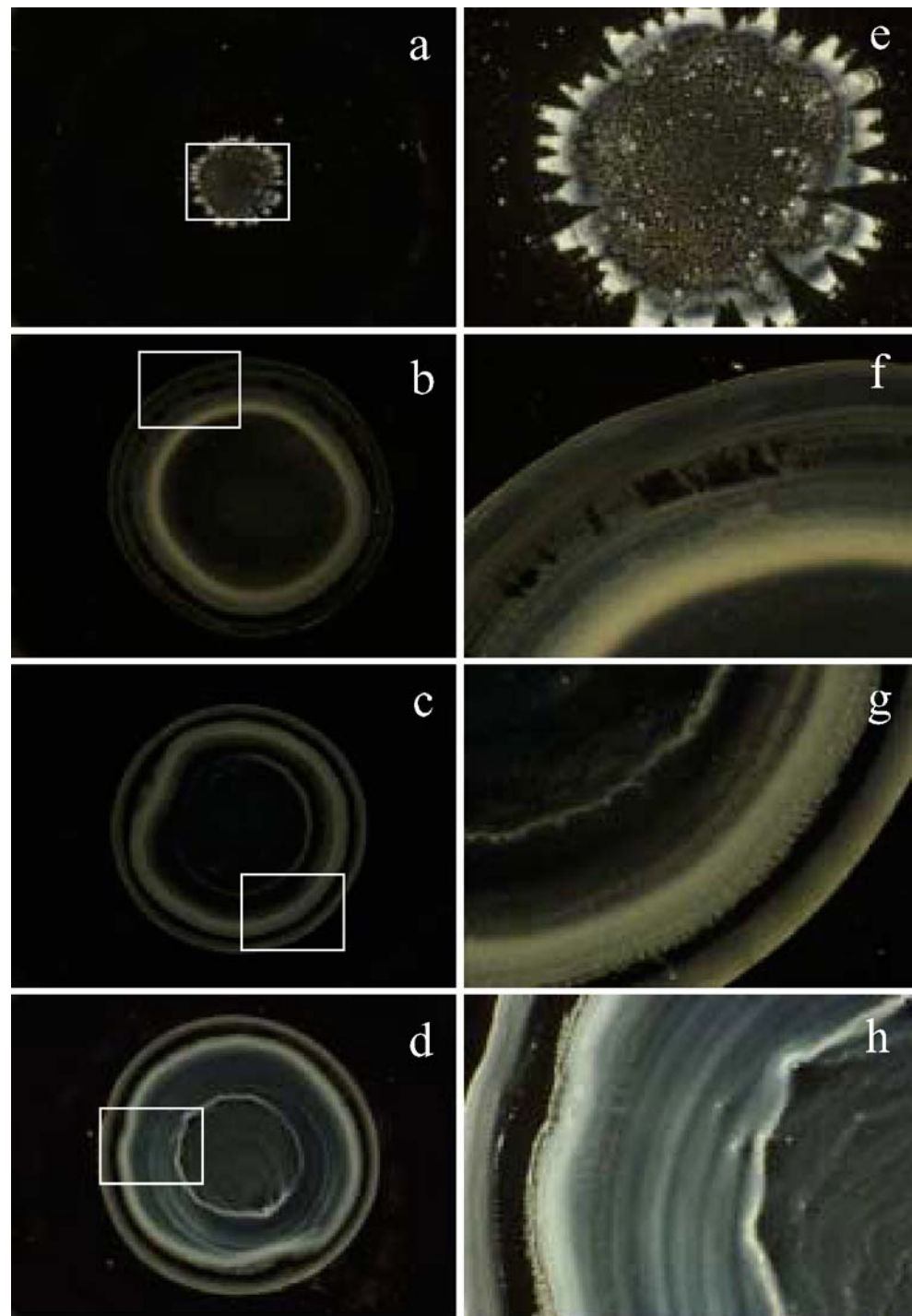
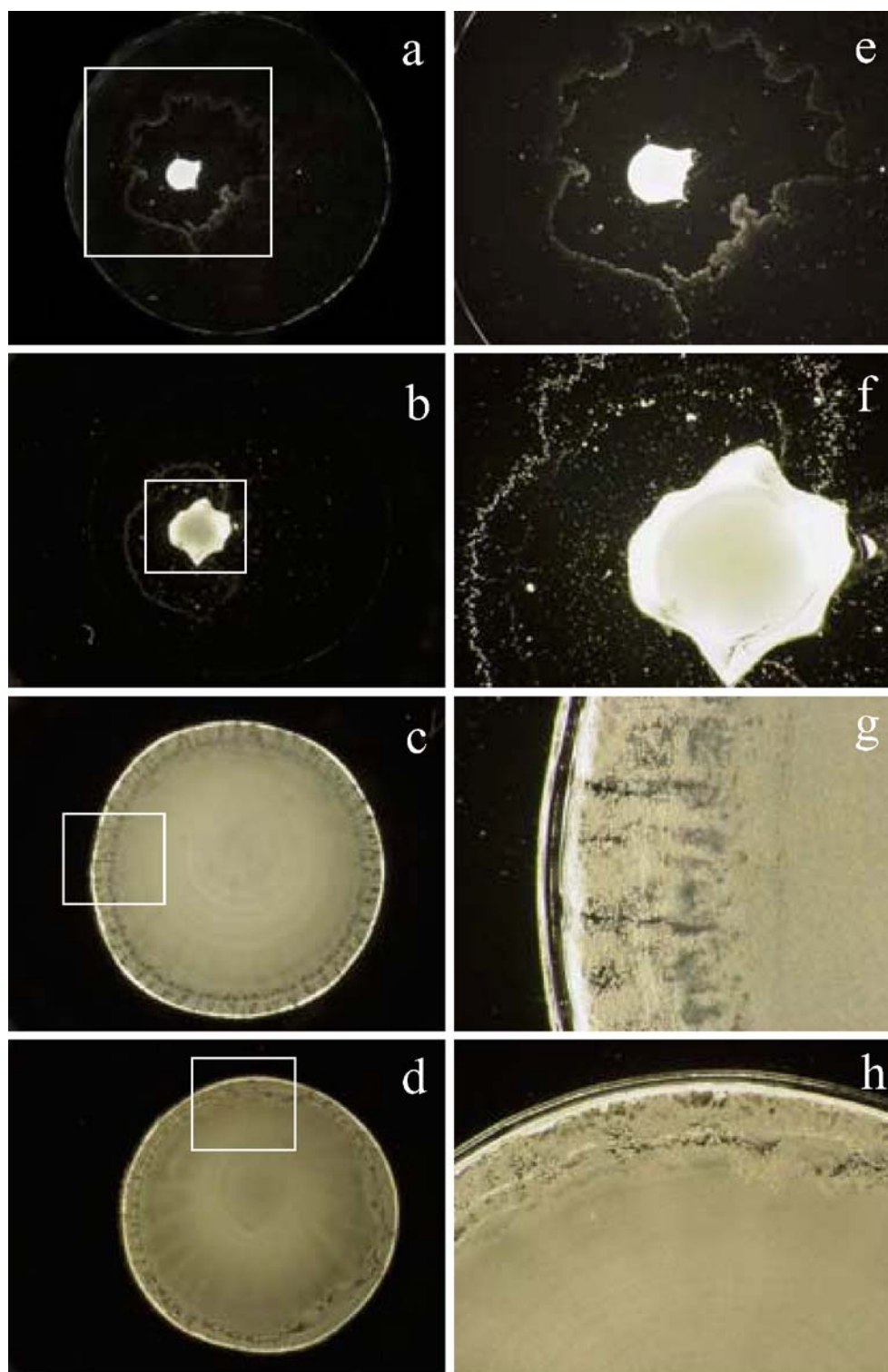


Figure 5 shows the drying patterns of PNIPAAm gels at $w=0.01$ g/ml and at various temperatures. Now, very beautiful patterns are observed both above and below the transition temperature 35 °C and they are undoubtedly due to the gravitational and Marangoni convectional flow of water and the gel spheres. Extension of the patterns above 35 °C was also observed very sharply. Below 35 °C,

multiple-broad rings formed. However, the thickest ring (ca. 30 μm at the peak) located at the outer edges, which was observed from the thickness measurements with a 3D-profile laser microscope VK-8500 (see Fig. 2g, for example). Furthermore, gel accumulation was observed at the central area and the shape was round with the height of ca. 6 μm at the central point below 35 °C. Above 35 °C, the

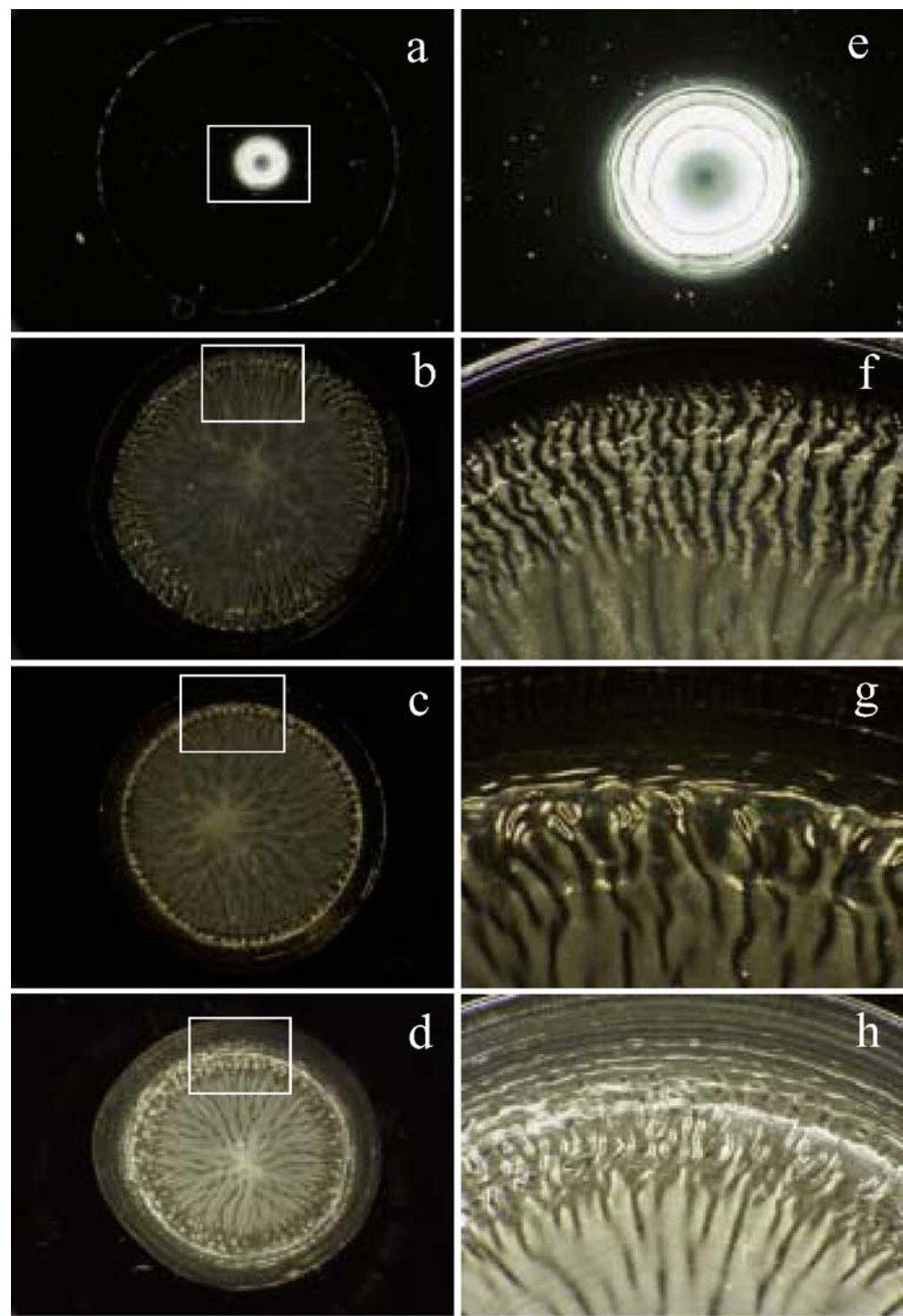
Fig. 4 Drying patterns of PNIPAAm at 25 °C. In water, 0.05 ml, $w=1.0\times 10^{-3}$ g/ml, **a** and **e** 25 °C, **b** and **f** 32 °C, **c** and **g** 35 °C, **d** and **h** 40 °C; length of the bar is 2.0 mm for **a**, **b**, **c**, and **d** and 0.5 mm for **e**, **f**, **g**, and **h**



flickering spoke-like patterns were observed, which are due to the traces of the convectational flow including cell convections, which were observed by T. Terada, for the first time, for Chinese ink on water surface [3–6]. It should be further noted in this study that the thicknesses

of the film around the central area were flat and ca. 5 μm , and that of the broad ring at the outside edges decreased when the temperature increased, though the picture showing these was omitted in this article. It should be mentioned in this study that the flickering spoke-like drying

Fig. 5 Drying patterns of PNIPAAm at 25 °C. In water, 0.05 ml, $w=0.01$ g/ml, **a** and **e** 25 °C, **b** and **f** 35 °C, **c** and **g** 40 °C, **d** and **h** 45 °C; length of the bar is 2.0 mm for **a**, **b**, **c** and **d** and 0.5 mm for **e**, **f**, **g**, and **h**



patterns show the traces of the cell convection of water and PNIPAAm, and somewhat viscous gel suspension, was helpful to memorize the cell convections in the drying processes.

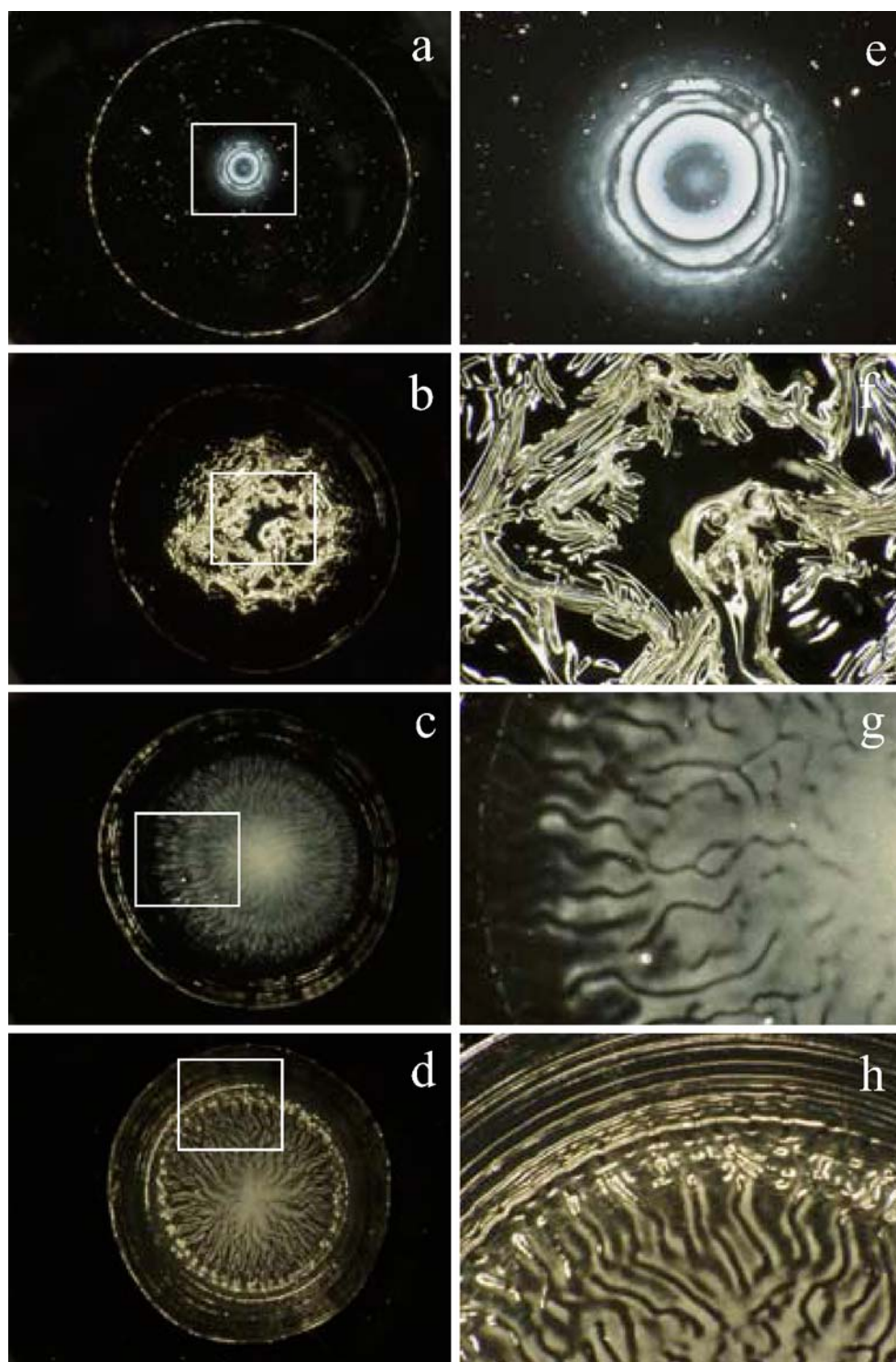
Figure 6 shows the drying patterns at $w=0.02$ g/ml, highest gel concentration among our experiments. It is interesting to note that highly fluctuated patterns were observed at the transition temperature, in this case at 32 °C

(see Fig. 6b,f). These patterns support strongly that the vigorous flow occurred in the suspension phase before the solidification.

Influence of salt concentration

Figures 7 and 8 show the drying patterns of PNIPAAm gels at the concentrations of 1×10^{-5} and 1×10^{-3} g/ml

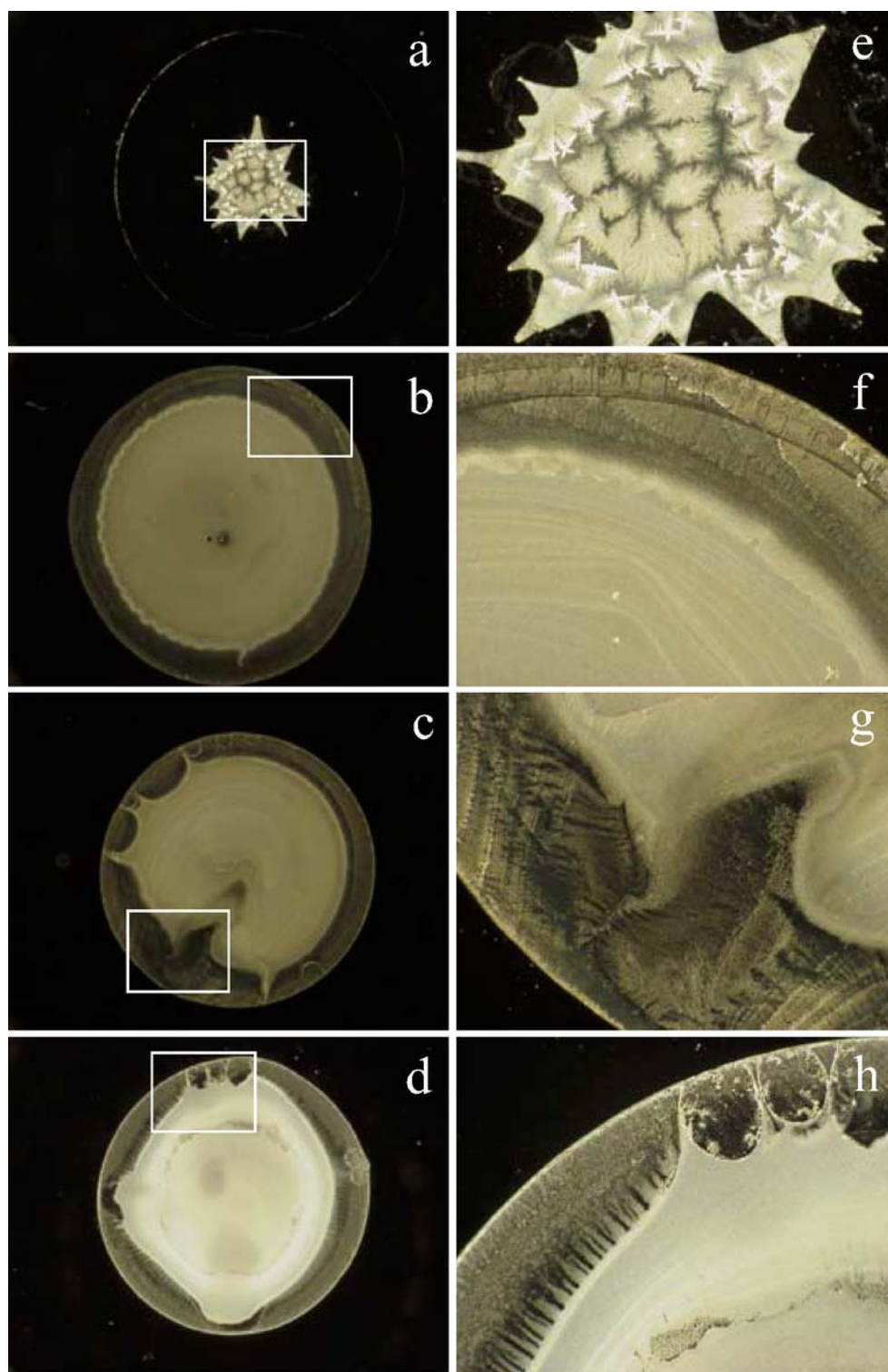
Fig. 6 Drying patterns of PNIPAAm at 25 °C. In water, 0.05 ml, $w=0.02$ g/ml, **a** and **e** 25 °C, **b** and **f** 32 °C, **c** and **g** 35 °C, **d** and **h** 40 °C; length of the bar is 2.0 mm for **a**, **b**, **c** and **d** and 0.5 mm for **e**, **f**, **g**, and **h**



when the concentrations of sodium chloride were 1×10^{-4} and 1×10^{-3} mol/l, respectively. Extension of the patterns above 35 °C took place between 0 to 1×10^{-3} mol/l irrespective of the salt concentration. However, the cooperative pattern formation of gels with NaCl was observed

irrespective of suspension temperature especially in the extended pictures. In subpanels e to h of Fig. 7, the cooperative patterns are clear, where black and white parts are gels and salt, respectively. It should be noted that the cooperative drying pattern formation has been demon-

Fig. 7 Drying patterns of PNIPAAm at 25 °C. In water, 0.05 ml, $w=1.0\times 10^{-5}$ g/ml, $[\text{NaCl}]=1.0\times 10^{-4}$ mol/l, **a** and **e** 25 °C, **b** and **f** 35 °C, **c** and **g** 40 °C, **d** and **h** 45 °C; length of the bar is 2.0 mm for **a**, **b**, **c** and **d** and 0.5 mm for **e**, **f**, **g**, and **h**

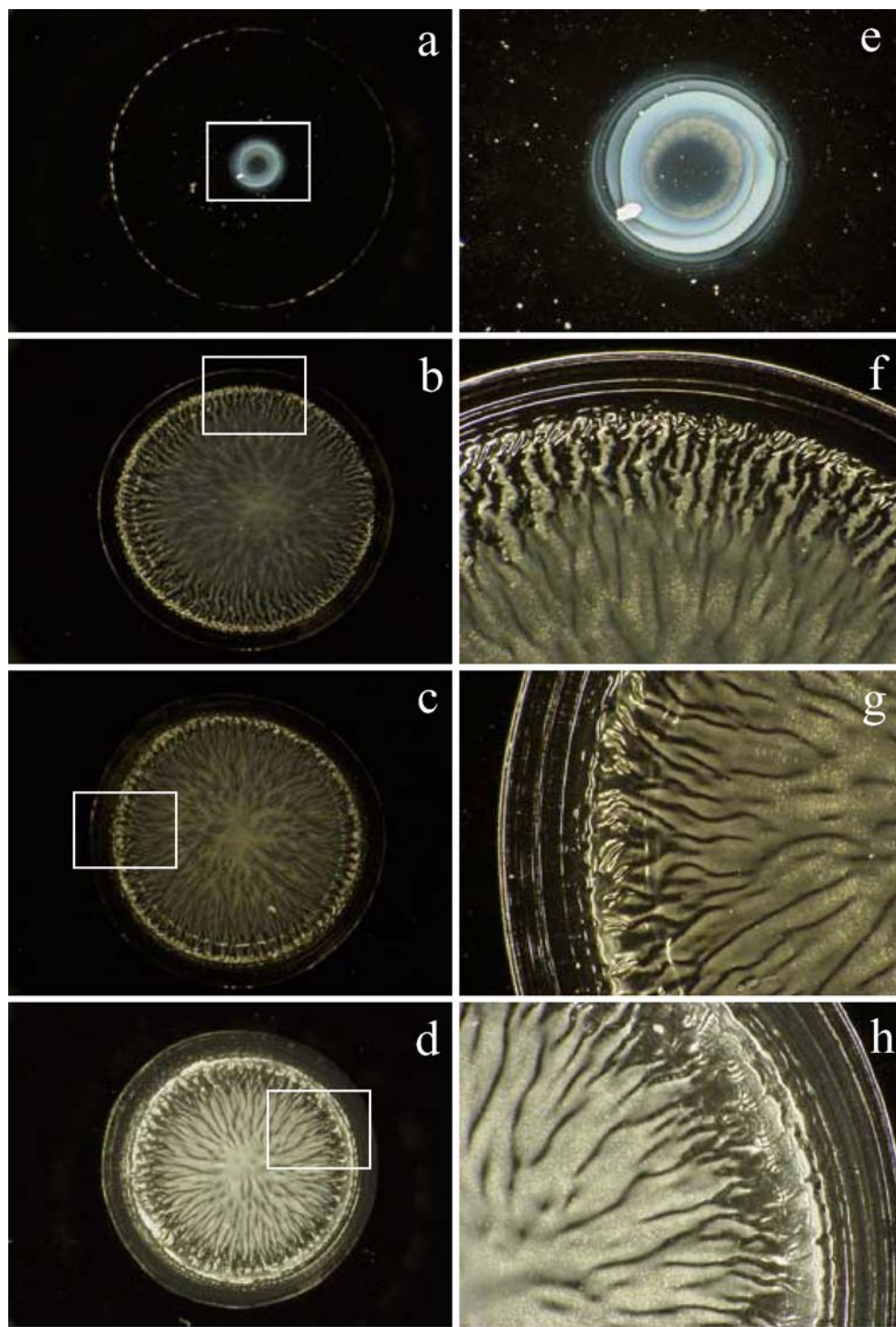


strated much more clearly for the mixtures of colloidal silica spheres and sodium chloride in a glass dish quite recently [16]. Discussion on why and how the cooperative pattern formation takes place is exciting and must

be made based on the detailed experimental results in near future.

The areas (S), covered with the gel particles in the dried film, at $w=1\times 10^{-5}$ g/ml increased sharply when

Fig. 8 Drying patterns of PNIPAAm at 25 °C. In water, 0.05 ml, $w=0.01$ g/ml, $[\text{NaCl}]=1.0\times 10^{-3}$ mol/l, **a** and **e** 25 °C, **b** and **f** 35 °C, **c** and **g** 40 °C, **d** and **h** 45 °C; length of the bar is 2.0 mm for **a**, **b**, **c** and **d** and 0.5 mm for **e**, **f**, **g**, and **h**



sodium chloride was added to the suspensions at 25 and 30 °C, whereas S was quite insensitive to the sodium chloride addition at high temperatures from 35 to 50 °C. It is interesting to note that at $w=0.01$ g/ml the S -values were quite insensitive to the salt concentration, though they decreased slightly from 60 to 55 mm² as

temperature increased from 25 to 50 °C. Furthermore, the drying time (T) from suspension state to the dried state at $w=1\times 10^{-5}$ g/ml decreased sharply from ca. 150 to 15 min as temperature increased from 25 to 50 °C. However, T kept constant irrespective of the salt concentrations.

References

1. Okubo T, Okuda S, Kimura H (2002) *Colloid Polym Sci* 280:454
2. Okubo T, Kimura K, Kimura H (2002) *Colloid Polym Sci* 280:1001
3. Terada T, Yamamoto R, Watanabe T (1934) *Sci Pap Inst Phys Chem Res Jpn* 27:173
4. Terada T, Yamamoto R, Watanabe T (1934) *Proc Imp Acad (Tokyo)* 10:10
5. Terada T, Yamamoto R, Watanabe T (1934) *Sci Pap Inst Phys Chem Res Jpn* 27:75
6. Terada T, Yamamoto R (1935) *Proc Imp Acad (Tokyo)* 11:214
7. Okubo T, Yamada T, Kimura K, Tsuchida A (2005) *Colloid Polym Sci* 283:1007
8. Okubo T, Kimura H, Kimura T, Hayakawa F, Shibata T, Kimura K (2005) *Colloid Polym Sci* 283:1
9. Yamaguchi T, Kimura K, Tsuchida A, Okubo T, Matsumoto M (2005) *Colloid Polym Sci* 283:1123
10. Okubo T, Kanayama S, Ogawa H, Hibino M, Kimura K (2004) *Colloid Polym Sci* 282:230
11. Okubo T, Yamada T, Kimura K, Tsuchida A (2006) *Colloid Polym Sci* 284:372
12. Okubo T, Kanayama S, Kimura K (2004) *Colloid Polym Sci* 282:486
13. Kimura K, Kanayama S, Tsuchida A, Okubo T (2005) *Colloid Polym Sci* 283:898
14. Okubo T, Shinoda C, Kimura K, Tsuchida A (2005) *Langmuir* 21:9889
15. Okubo T (2006) *Colloid Polym Sci* 284:1191
16. Okubo T (2006) *Colloid Polym Sci* 284:1395
17. Okubo T (2006) *Colloid Polym Sci* (in press) DOI [10.1007/s00396-006-1576-6](https://doi.org/10.1007/s00396-006-1576-6)
18. Okubo T (2006) *Colloid Polym Sci* (in press) DOI [10.1007/s00396-006-1555-y](https://doi.org/10.1007/s00396-006-1555-y)
19. Hu Z, Lu X, Gao J (2001) *Adv Mater* 13:1708
20. Ito S, Ogawa K, Suzuki H, Wang B, Yoshida R, Kokufuta E (1999) *Langmuir* 15:4289
21. Okubo T, Hase H, Kimura H, Kokufuta E (2002) *Langmuir* 18:6783
22. Ohara PC, Heath JR, Gelbart WM (1997) *Angew Chem* 109:1120
23. Ohara PC, Heath JR, Gelbart WM (1998) *Langmuir* 14:3418
24. Gelbart WM, Sear RP, Heath JR, Chang S (1999) *Faraday Discuss* 112:299